



## Investigation of Chemical Modification and Enzymatic Degradation of Poly(vinyl alcohol)/Hemoprotein Particle Composites

Sameer Awad  

Department of Chemistry, College of Education for Pure Science, University of Anbar-Iraq.

**Abstract:** Polyvinyl alcohol (PVA) composite films with different hemp protein particles (HPP) as additives were successfully synthesized by a solution casting method. The properties of HPP-based PVA composite films were investigated. The characterizations of pure PVA and PVA composite films were performed regarding Fourier transform infrared spectroscopy (FTIR), ultra-violet (UV-Vis) to investigate the chemical properties. The formation of hydrogen bond in the PVA-HPP films, which could improve the compatibility of the two components was investigated by FTIR spectroscopy and UV-Vis analysis. The overall results showed that a higher loading of HPP into the PVA matrix improved the chemical interactions significantly. The swelling degree decreased while the water contact angle values increased as the HPP content increased.

**Keywords:** Polyvinyl alcohol, hemp protein, composites, chemical modification, enzymatic degradation

**Submitted:** February 11, 2021. **Accepted:** May 07, 2021.

**Cite this:** Awad S. Investigation of chemical modification and enzymatic degradation of poly (vinyl alcohol)/hemoprotein particle composites. JOTCSA. 2021;8(2):651-8.

**DOI:** <https://doi.org/10.18596/jotcsa.878495>.

**\*Corresponding author. E-mail:** [Sameer.msc1981@gmail.com](mailto:Sameer.msc1981@gmail.com).

### INTRODUCTION

Production of biodegradable material from natural materials resources instead of non-biodegradable synthetic polymers increases great attention due to the developing consciousness of the green environment (1-4). Several researchers have synthesized biodegradation composites, applying many forms of natural polymers as fillers such as cellulose, lignin, starch, chitin, chitosan, soy protein, and wheat protein. These fillers were used as bioabsorbable composites due to their low cost, excellent processability, biodegradability, and simplicity of physical and chemical improvements (5,6).

Generally, the natural materials as additives, which revealed are difficult to melt or dissolve in a normal solvent procedure as a result of their strong intermolecular bonding between cellulose and lignin even though the abundance of these natural materials (6). Hence, the addition of the synthetic polymer is regularly studied to convert these into an expected form. While these materials are significant

mainly due to their environmentally friendly nature, to prepare a completely green material, the biodegradable synthetic polymer's utilities are more advantageous rather than the non-biodegradable (7-9).

PVA is considered a great low-cost option because it is recognized for its chemical, thermal stability, and biodegradability. Renewable fillers (carbohydrates and fibers) are cheap and biodegradable naturally in the environment (10). Many plant materials are derived from renewable crops or their wastes processed, adding a good source of fibers for many industrial applications (11-14). The hydrophilic composition, which consists of hydroxyl groups in the PVA structure, is well-linked with carbohydrates, creating significant agreement in composites (15-18).

Fiber-reinforced polymer matrix became substantial attention in many applications as a result of the good properties and superior advantages of natural fiber in term of its relatively low weight, low cost,

less damage to processing equipment, and good relative mechanical properties (19).

This study was investigated based on the chemical and HPP biodegradation treatment, defibrillated and distributed in an aqueous suspension. The films of PVA/HPP composite were prepared by the casting method. PVA-HPP films containing different HPP loadings of 3, 7, and 12% (w/w), were formed as composites. The chemical, biological, and physical characterizations were assessed. The purpose of this work was to assess the impact of incorporating HPP addition in PVA films, evaluating their compositions, chemical and biodegradation characterizations of PVA composites.

## EXPERIMENTAL

### Materials

Polyvinyl alcohol material was provided from Sigma-Aldrich, UK, MW= 124,000-186,000; the hydrolysis degree is in the range 87-89 mol%; hydrolysis rate: 90%; density: 1.3 g/cm<sup>3</sup>. The  $\alpha$ -amylase and  $\beta$ -amylase were provided from Merck KGaA Co.

Germany. Hemp protein particles were purchased locally, containing 1.7% moisture, 0.23% protein and 0.075% fat, and used without further chemical treatments.

### PVA Composite Preparations

A 7% (w/v) PVA solution was prepared by inserting 10 g of PVA into 90 mL of distilled water. Then, the solution was heated and stirred at ~80 °C for 6 hours to achieve complete homogeneity, after that the solution was kept at room temperature. The 10% (w/v) PVA solution was mixed with 3, 7, and 12% of HPP powder (HPP particle size 300  $\mu$ m), creating the casting solution. The composite mixture was poured into a glass dish and positioned on a levelled smooth surface with the right thickness (40  $\mu$ m). The composite mixture was kept for three days at room temperature and then by drying in a vacuum oven at 60 °C for three days. After drying, the composite films were later removed from their dishes and put up in a desiccator for future use. Figure 1 shows the chemical covalent interaction between HPP and PVA to form PVA composites.

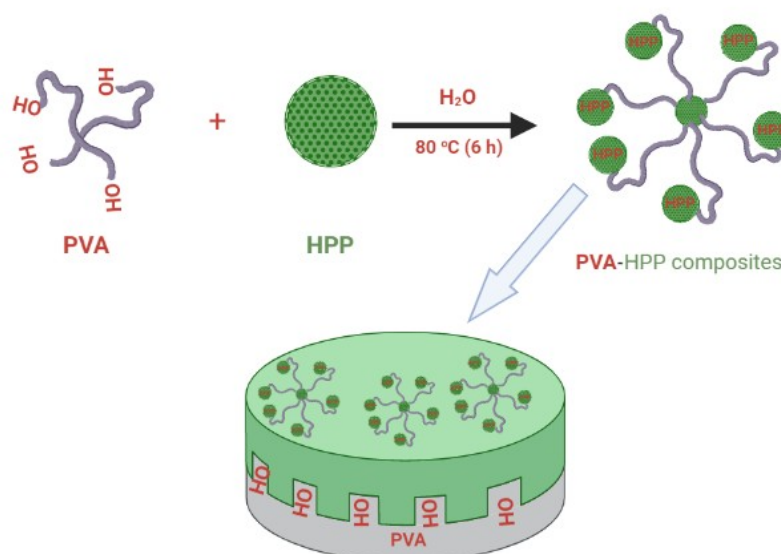


**Figure 1:** Chemical covalent interaction between HPP and PVA to form PVA composites.

## CHARACTERIZATION

### Fourier Transform Infrared Spectroscopic analysis

FT-IR analysis of composite films was carried out utilizing an FTIR Spectrum 400 (Perkin Elmer, USA). The investigation was performed within the range between 4000 to 500 cm<sup>-1</sup> with a 4 cm<sup>-1</sup> resolution and a total of 20 scans. The spectra of FTIR were recorded in the absorbance mode.

### UV-VIS Analysis

A UV-Visible-NIR spectrometer was utilized a double beam Lambda-25 UV-VIS spectrophotometer

(Bandwidth: 1 nm and minimum spectral resolution: 0.5 nm) to determine the maximum absorbance spectra within the wavelength range (200 to 700 nm).

### X-Ray Diffraction

The XRD test for all samples was carried out utilizing an X-ray spectrometer model a (PANalytical, USA) at a scan rate (0.02° s<sup>-1</sup>) and the 2 $\theta$  range were between 0 and 80. The wavelength of the X-ray was 1.5 Å with a radiation source (CuK $\alpha$ ). All samples were conducted at 40 kV and 15 mA.

### Swelling Degree (SD) and Contact Angle Analysis

PVA and PVA composite samples were cut off into pieces of 3 × 3 cm, weighed, and immersed in deionized water at 25 °C for 60 days with different crosslinking times. The swollen sample was taken out and wiped with tissue paper to eliminate the residual water on the surface of the film and then weighed. The swelling degree is calculated by utilizing the following equation.

$$SD(\%) = \frac{W_s - W_D}{W_D} \times 100 \quad (\text{Eq. 1})$$

Where  $W_s$  = the weight of swollen samples,  $W_D$  = the weight of dried specimens.

The water contact angle values were tested of PVA composites, using an optical contact angle meter type (SL200KB, USA) to support the surface hydrophilicity of samples.

### Enzymatic Testing

Specific quantities of  $\alpha$ -amylase,  $\beta$ -amylase, and distilled water form an enzymatic mixture placed in a plastic test tube. The films were cut to species with dimensions (2×2 cm<sup>2</sup>), and then, they were weighed by utilizing a digital sensitive balance. The samples were immersed in plastic test tubes and subjected to a shaking incubator at a rate of speed 100 rpm at 27 °C and kept for 120 h. Any residual enzyme mixture was removed, washed, utilizing distilled water. The samples were dried in a desiccator under vacuum for 48 h, and then they were weighted. The degree of enzymatic

degradation [DED %] was accounted based on the following equation.

$$DED(\%) = \frac{W_D - W_I}{W_D} \times 100 \quad (\text{Eq. 2})$$

Where  $W_D$  = the dry weight of the samples after the enzymatic treatment,  $W_I$  = the initial dry weight of the samples,

## RESULTS AND DISCUSSION

### FT-IR Analysis: Chemical Linkage

The FT-IR spectra of the PVA and PVA/HPP composites are shown in Figure 2. PVA showed a wide-ranging peak at 3500–3600 cm<sup>-1</sup> that is attributable to O-H stretching. The specific peaks at 2850 cm<sup>-1</sup>, 1400 cm<sup>-1</sup> and 1100 cm<sup>-1</sup> were attributed to C-H stretching, C-H bending and C-O stretching, respectively. In the FT-IR absorbance spectra of PVA and PVA/HPP, the band at 2854 cm<sup>-1</sup> involves the stretching of the C-H bond in the crosslinked PVA and PVA/HP composites be attributed to the alkyl chain of aldehydes. The bands observed at 1100–1145 cm<sup>-1</sup>. Similar groups seem in 2935/2905 cm<sup>-1</sup>, instead of CH<sub>2</sub> asymmetric and symmetric stretching; 1605 cm<sup>-1</sup> is the C-O vibration and 1435 cm<sup>-1</sup> due to CH<sub>2</sub> bending. The broad groups between 3000–3500 cm<sup>-1</sup>, which are related to the stretching vibration of the hydroxyl group, display the presence of intermolecular, intramolecular hydrogen bands, and the reduced band intensity after the increase of HPP loading in PVA and gave higher crosslinking that indicated the formation of the hydroxyl group.

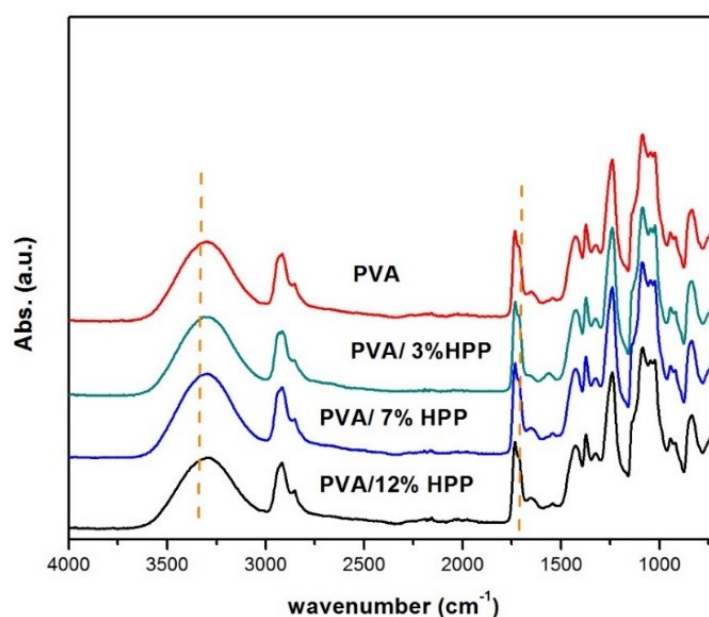
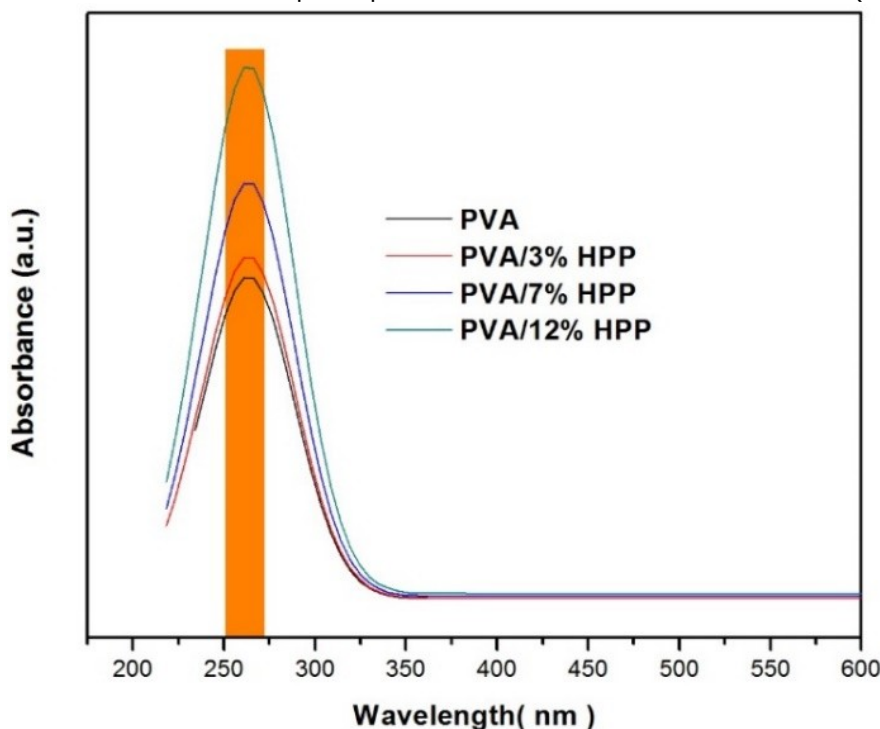


Figure 2: FTIR Spectra of PVA and PVA composites.

### UV Absorption

Figure 3 shows the UV-vis absorption of the PVA with different HPP loading. The UV absorption of PVA-HPP composites showed an absorption peak at 260 nm corresponding to  $n \rightarrow \pi^*$  transition of HPP filler. Pure HPP represented an absorption at about 260 nm related to its chromophoric groups. In addition, pure PVA did not show any absorption peak in the range of 200–600 nm. As it is shown in Figure 3, pure PVA-HPP shows an absorption peak

related to HPP absorption peak. After incorporation of HPP in the PVA matrix, the peak shifted to higher absorption which indicates the interaction between HPP and PVA matrix. The minimal absorption of PVA showed that the PVA has a clarity characteristic. In the UV region (200-400 nm), the pure PVA displayed weak UV blocking as a result of the low light absorption. The intensity of UV absorption of PVA raised greatly as the amount of HPP rose from 3 to 12 wt.% in the PVA matrix (Figure 3).



**Figure 3:** UV-Vis absorption spectra of PVA and PVA/HPP composite samples with different loadings of HPP.

### X-ray Diffraction

X-ray diffraction was carried out to test the PVA nature and PVA composites' crystallinity. Figure 4 illustrates the diffraction pattern for the PVA and PVA/HPP composites, as shown clearly in Figure 8, a broad peak at  $2\theta = 17.5^\circ$  (peak 1) for the pure PVA film. However, it was also obviously noticed that the PVA composite intensity exhibited higher values and significantly shifted toward the higher value of the angles as the HPP additives were increased. Thus, it indicates that incorporating HPP additives into the PVA matrix significantly increased the amorphous region domain. When the PVA composite becomes much amorphous, it can be enhanced by reducing

the PVA composite relative crystallization. As shown in the XRD spectra of PVA, there were two peaks around  $2\theta = 11.0^\circ$  and  $2\theta = 19.5^\circ$  (16). From Figure 4, it is shown that as the content of HPP was increased from 3 wt. % to 12 wt. % in PVA, the peak at  $2\theta = 18.2^\circ$  slightly increased to  $2\theta = 20.6^\circ$ . Therefore, these diffractograms proposed that HPP in PVA has included a combination of crystalline and amorphous peaks (20). These results also indicate that the addition of HPP does not affect the uniformity in the blended PVA matrix structure. However, rather enhance molecular ordering in the amorphous phase of the PVA matrix (21).

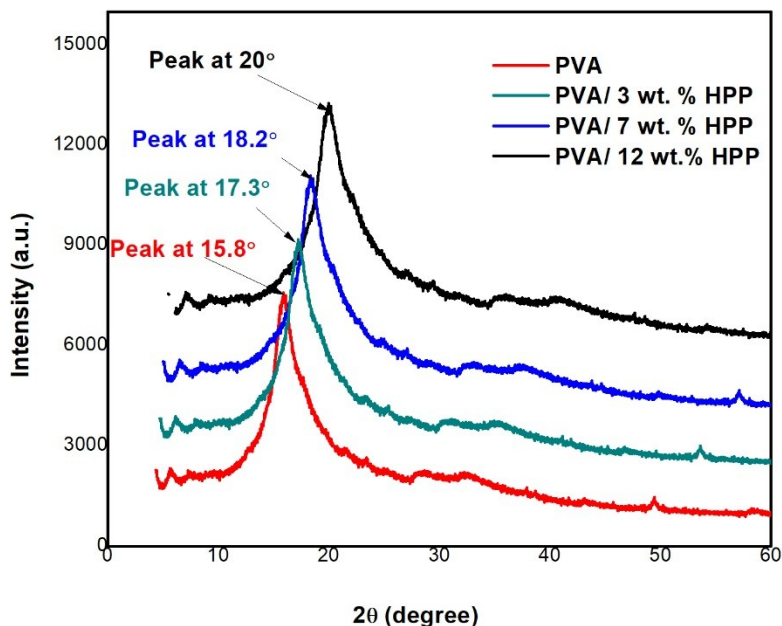


**Figure 4.** XRD spectra for PVA and PVA/HPP composites with different loadings of HPP.

#### Effect of the Water Uptake on the Properties of PVA/HPP Composites

The wetting behavior of PVA composites was investigated by the static angle with a contact angle meter by drop method. It was analyzed that neat PVA is hydrophilic with a contact angle of  $48.8^\circ$  as shown in Figure 5 A. However, the water contact angle of PVA composites was reduced as the concentration of HNT nanoparticles was increased. The 12 wt.% of HNT in the PVA matrix have the highest hydrophobicity with a contact angle of  $83^\circ$  while the water contact angle 3 and 7 wt.% HNT in PVA increased slightly in comparison to that of pure PVA ( $48.8^\circ$ ) as shown in Figure 5(A).

The value of water absorption in terms of swelling percentage crosslinked PVA and PVA composite samples are shown in Figure 5.B.

PVA has a higher value of swelling percentage of 82% due to the presence of a large number of hydroxy groups. These hydroxyl groups allow incoming water to occur in the interspaces between mobile polymer chains in the amorphous region of polymer and hence cause large swelling. In crosslink films, a smaller number of hydroxyl groups and restricted chain movement results in significantly lower water absorption compared to PVA (21-24).

In composite films, crosslinking of PVA-12% HPP also demonstrates a significant lowering in the water absorption of PVA (52.8%) while 3 and 7 wt% of HNT loading showed slightly decreased by 72.5% and 67.5%, respectively, which is slightly better than the swelling percentage of PVA (82.5%). This is because the crosslinked PVA with HPP is less hydrophilic and absorbs less water.

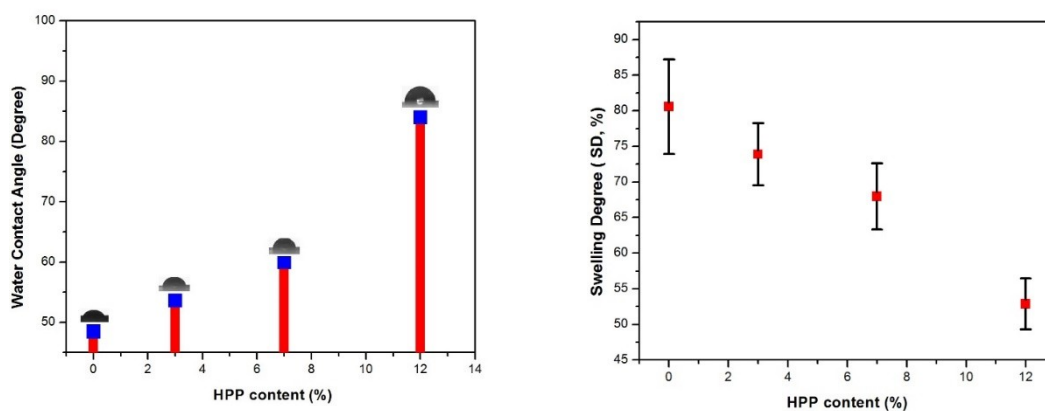


**Figure 5:** The water contact angle (left) and swelling degree (right) of PVA and PVA/HPP composites.

#### Enzymatic Testing

The weight loss of pure PVA and PVA composites is displayed in Figure 6. The percentage of DED was

accounted for later the PVA composites had been immersed in enzymatic solution up to 100 h. The degree of enzymatic degradation (DED, %) was

increased with increasing the enzymatic treatment times, as shown in Figure 6. With the addition of the biodegradable HPP, the PVA blends became much easier to degrade, as shown in Figure 6. After 20 h immersion time, the degree of enzymatic degradation of PVA composites increased slightly in comparison to the PVA matrix. The DED, % of PVA increased up to 64.2% while (DED, %) values of 3, 7, and 12 wt.% HP in PVA was 26, 30, and 37.4%, respectively. Pure PVA exhibited a slower rate of

degradation than PVA composites. After 100 h immersion treatment time, 12 wt. % of HPP in PVA exhibited a higher enzymatic degradation rate (95.5%) while the pure PVA was 67.5%. This higher observation of the amylase solution in PVA/12 wt.% HPP the film was due to the hydroxyl group that enhanced the diffusion of  $\alpha$  amylase and  $\beta$ -amylase into the PVA/HPP composite films and then improved the attack of amylase on the HPP.

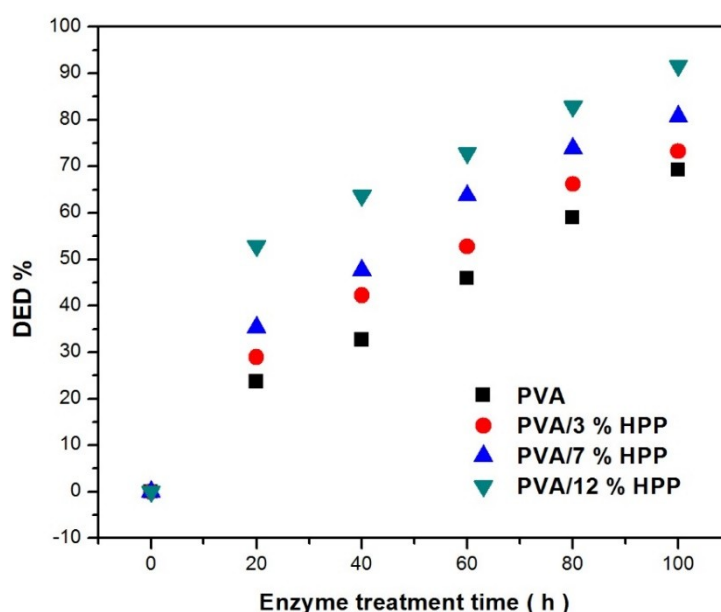


**Figure 6:** Enzymatic biodegradation of PVA and PVA/HPP composite films using  $\alpha$ -amylase and  $\beta$ -amylase.

## CONCLUSIONS

HPP has been used as reinforcement in the PVA matrix and prepared with sample solution casting. There is a remarkable improvement in chemical interaction that noticed in FT-IR and UV-VIS spectral analyses. The chemical stability was enhanced with increasing HPP loading. The overall results showed that a higher loading of HPP into the PVA matrix improved the chemical interactions significantly. The swelling coefficient decreased while the water contact angle values increased as the HPP content increased. From the XRD results, crystallinity was decreased by incorporating HPP in the PVA matrix. The degree of enzymatic degradation (DED, %) was increased with increasing the enzymatic treatment times of PVA composites and swelling degree decreased with increasing HPP loading in the PVA matrix. Overall, an environmentally friendly technique was investigated to HPP in wide applications such as biodegradable packaging.

## REFERENCES

1. Silva EL da, Reis CA, Vieira HC, Santos JX dos, Nisgoski S, Saul CK, et al. Evaluation Of Poly(Vinyl Alcohol) Addition Effect On Nanofibrillated Cellulose

Films Characteristics. CERNE. 2020 Mar;26(1):1-8. Doi:

<https://doi.org/10.1590/01047760202026012654>.

2. Mendes JF, Paschoalin RT, Carmona VB, Sena Neto AR, Marques ACP, Marconcini JM, et al. Biodegradable polymer blends based on corn starch and thermoplastic chitosan processed by extrusion. Carbohydrate Polymers. 2016 Feb;137:452-8. Doi: <https://doi.org/10.1016/j.carbpol.2015.10.093>.

3. Haque ANMA, Remadevi R, Wang X, Naebe M. Biodegradable cotton gin trash/poly(vinyl alcohol) composite plastic: Effect of particle size on physicochemical properties. Powder Technology. 2020 Sep;375:1-10. Doi: <https://doi.org/10.1016/j.powtec.2020.07.096>.

4. Tan B, Ching Y, Poh S, Abdullah L, Gan S. A Review of Natural Fiber Reinforced Poly(Vinyl Alcohol) Based Composites: Application and Opportunity. Polymers. 2015 Nov 2;7(11):2205-22. Doi: <https://doi.org/10.3390/polym7111509>.

5. Guirguis OW, Moselhey MTH. Thermal and structural studies of poly (vinyl alcohol) and hydroxypropyl cellulose blends. NS.

- 2012;04(01):57–67. Doi: <https://doi.org/10.4236/ns.2012.41009>.
6. Eaysmine S, Haque P, Ferdous T, Gafur MA, Rahman MM. Potato starch-reinforced poly(vinyl alcohol) and poly(lactic acid) composites for biomedical applications. *Journal of Thermoplastic Composite Materials*. 2016 Nov;29(11):1536–53. Doi: <https://doi.org/10.1177/0892705715569824>.
7. Julinová M, Kupec J, Alexy P, Hoffmann J, Sedlařík V, Vojtek T, et al. Lignin and starch as potential inductors for biodegradation of films based on poly(vinyl alcohol) and protein hydrolysate. *Polymer Degradation and Stability*. 2010 Feb;95(2):225–33. Doi: <https://doi.org/10.1016/j.polymdegradstab.2009.10.008>.
8. Gadhavé RV, S. K. V, Mahanwar PA, Gadekar PT. Effect of addition of boric acid on thermo-mechanical properties of microcrystalline cellulose/polyvinyl alcohol blend and applicability as wood adhesive. *Journal of Adhesion Science and Technology*. 2020 Oct 20;1–15. Doi: <https://doi.org/10.1080/01694243.2020.1832775>.
9. Awad SA, Khalaf EM. Evaluation of the photostabilizing efficiency of polyvinyl alcohol–zinc chloride composites. *Journal of Thermoplastic Composite Materials*. 2020 Jan;33(1):69–84. Doi: <https://doi.org/10.1177/0892705718804585>.
10. Mok CF, Ching YC, Muhamad F, Abu Osman NA, Singh R. Poly(vinyl alcohol)- $\alpha$ -chitin composites reinforced by oil palm empty fruit bunch fiber-derived nanocellulose. *International Journal of Polymer Analysis and Characterization*. 2017 May 19;22(4):294–304. Doi: <https://doi.org/10.1080/1023666X.2017.1288345>.
11. Jensen B, Kepley W, Guarner J, Anderson K, Anderson D, Clairmont J, et al. Comparison of Polyvinyl Alcohol Fixative with Three Less Hazardous Fixatives for Detection and Identification of Intestinal Parasites. *Journal of Clinical Microbiology*. 2000;38(4):1592–8. Doi: <https://doi.org/10.1128/JCM.38.4.1592-1598.2000>.
12. Oviedo IR, Méndez NAN, Gómez MPG, Rodríguez HC, Martínez AR. Design of a Physical and Nontoxic Crosslinked Poly(Vinyl Alcohol) Hydrogel. *International Journal of Polymeric Materials*. 2008 Oct 13;57(12):1095–103. Doi: <https://doi.org/10.1080/00914030802341661>.
13. Kobayashi M, Hyu HS. Development and Evaluation of Polyvinyl Alcohol-Hydrogels as an Artificial Articular Cartilage for Orthopedic Implants. *Materials*. 2010 Apr 14;3(4):2753–71. Doi: <https://doi.org/10.3390/ma3042753>.
14. Pervez Md, Stylios G. Investigating the Synthesis and Characterization of a Novel “Green” H<sub>2</sub>O<sub>2</sub>-Assisted, Water-Soluble Chitosan/Polyvinyl Alcohol Nanofiber for Environmental End Uses. *Nanomaterials*. 2018 Jun 1;8(6):395. <https://doi.org/10.3390/nano8060395>.
15. Salleh MSN, Nor NNM, Mohd N, Draman SFS. Water resistance and thermal properties of polyvinyl alcohol-starch fiber blend film. In Istanbul, Turkey; 2017 [cited 2021 May 7]. p. 020045. Available from: <http://aip.scitation.org/doi/abs/10.1063/1.4975460>
16. Wan W, Bannerman AD, Yang L, Mak H. Poly(Vinyl Alcohol) Cryogels for Biomedical Applications. In: Okay O, editor. *Polymeric Cryogels* [Internet]. Cham: Springer International Publishing; 2014 [cited 2021 May 7]. p. 283–321. (Advances in Polymer Science; vol. 263). Available from: [http://link.springer.com/10.1007/978-3-319-05846-7\\_8](http://link.springer.com/10.1007/978-3-319-05846-7_8)
17. Awad SA, Khalaf EM. Investigation of Photodegradation Preventing of Polyvinyl Alcohol/Nanoclay Composites. *J Polym Environ*. 2019 Sep;27(9):1908–17. Doi: <https://doi.org/10.1007/s10924-019-01470-7>.
18. Imam SH, Cinelli P, Gordon SH, Chiellini E. Characterization of Biodegradable Composite Films Prepared from Blends of Poly(Vinyl Alcohol), Cornstarch, and Lignocellulosic Fiber. *J Polym Environ*. 2005 Jan;13(1):47–55. Doi: <https://doi.org/10.1007/s10924-004-1215-6>.
19. Awad SA, Khalaf EM. Investigation of improvement of properties of polypropylene modified by nano silica composites. 2019; 12: 59-63. Doi: <https://doi.org/10.1016/j.coco.2018.12.008>.
20. Lawton JW, Fanta GF. Glycerol-plasticized films prepared from starch–poly(vinyl alcohol) mixtures: effect of poly(ethylene-co-acrylic acid). *Carbohydrate Polymers*. 1994 Jan;23(4):275–80. Doi: [https://doi.org/10.1016/0144-8617\(94\)90190-2](https://doi.org/10.1016/0144-8617(94)90190-2).
21. Bodin A, Ahrenstedt L, Fink H, Brumer H, Risberg B, Gatenholm P. Modification of Nanocellulose with a Xyloglucan–RGD Conjugate Enhances Adhesion and Proliferation of Endothelial Cells: Implications for Tissue Engineering. *Biomacromolecules*. 2007 Dec 1;8(12):3697–704. Doi: <https://doi.org/10.1021/bm070343q>.
22. Awad SA. Mechanical and thermal characterisations of low-density polyethylene/nanoclay composites. *Polymers and Polymer Composites* 2020: 0967391120968441. Doi: <https://doi.org/10.1177/0967391120968441>.

23. Awad SA, Khalaf EM. Characterization and modifications of low-density polyethylene-nano cellulose composites. Suranaree Journal of Science&Technology. 2020; 27(1): 1-6.

24. Awad SA, Khalaf EM. Improvement of the chemical, thermal, mechanical and morphological properties of polyethylene terephthalate-graphene particle composites. Bulletin of Materials Science. 2018; 41: 1-6. Doi: <https://doi.org/10.1007/s12034-018-1587-1>.